Journal of Experimental Botany, Vol. 64, No. 7, pp. 1967–1981, 2013
doi:10.1093/jxb/ert056 Advance Access publication 6 April, 2013
This paper is available online free of all access charges (see http://jxb.oxfordjournals.org/open_access.html for further details)

Journal of Experimental Botany
www.jxb.oxfordjournals.org

RESEARCH PAPER

CAROTENOID CLEAVAGE DIOXYGENASE 7 modulates plant growth, reproduction, senescence, and determinate nodulation in the model legume *Lotus japonicus*

Junwei Liu[1], Mara Novero[2], Tatsiana Charnikhova[3], Alessandra Ferrandino[1], Andrea Schubert[1], Carolien Ruyter-Spira[3], Paola Bonfante[2], Claudio Lovisolo[1], Harro J. Bouwmeester[3] and Francesca Cardinale[1,*]

[1] Department of Agriculture, Forestry and Food Sciences, University of Turin, via Leonardo da Vinci 44, 10095 Grugliasco (TO), Italy
[2] Department of Life Sciences and Systems Biology, University of Turin, viale Mattioli 25, 10025 Turin, Italy
[3] Laboratory of Plant Physiology, Wageningen University, Droevendaalsesteeg 1, NL-6708 PB Wageningen, The Netherlands

*To whom correspondence should be addressed. E-mail: francesca.cardinale@unito.it

Received 21 November 2012; Revised 25 January 2013; Accepted 14 February 2013

Abstract

Strigolactones (SLs) are newly identified hormones that regulate multiple aspects of plant development, infection by parasitic weeds, and mutualistic symbiosis in the roots. In this study, the role of SLs was studied for the first time in the model plant *Lotus japonicus* using transgenic lines silenced for *CAROTENOID CLEAVAGE DIOXYGENASE 7* (*LjCCD7*), the orthologue of *Arabidopsis More Axillary Growth 3*. Transgenic *LjCCD7*-silenced plants displayed reduced height due to shorter internodes, and more branched shoots and roots than the controls, and an increase in total plant biomass, while their root:shoot ratio remained unchanged. Moreover, these lines had longer primary roots, delayed senescence, and reduced flower/pod numbers from the third round of flower and pod setting onwards. Only a mild reduction in determinate nodule numbers and hardly any impact on the colonization by arbuscular mycorrhizal fungi were observed. The results show that the impairment of CCD7 activity in *L. japonicus* leads to a phenotype linked to SL functions, but with specific features possibly due to the peculiar developmental pattern of this plant species. It is believed that the data also link determinate nodulation, plant reproduction, and senescence to CCD7 function for the first time.

Key words: Arbuscular mycorrhizal fungi (AMF), carotenoid cleavage dioxygenase, determinate nodulation, leaf senescence, *Lotus japonicus*, reproduction, shoot and root branching; strigolactone.

Introduction

Plant development is plastic and environmentally sensitive, and is regulated by hormones acting as long-range signals to integrate developmental, genetic, and environmental inputs. In the control of shoot and root branching, for example, large variations in plant architecture can be generated in a single genotype in response to a number of cues (Domagalska and Leyser, 2011; Müller and Leyser, 2011). The role of classic plant hormones, such as auxin and cytokinins, in the regulation of shoot and root branching and in the maintenance of coordinated growth between root and shoot has been extensively studied (Sachs, 2005; Hwang *et al*., 2012). Recently, strigolactones (SLs) have been identified as a new class of branch-inhibiting hormones that seem to fine-tune the regulation of shoot branching further (Gomez-Roldan *et al*., 2008; Umehara *et al*., 2008; Xie *et al*., 2010). In the past decade, genotypes affected in the SL pathway were identified, and include *ramosus* (*rms*) mutants in pea, *decreased apical dominance* (*dad*) in petunia, *more axillary branch* (*max*) in *Arabidopsis*, and *high-tillering dwarf* (*htd* or *d*) in rice (Beveridge and Kyozuka, 2009).

Besides regulating shoot architecture, SLs contribute to shaping the root system, by affecting primary root length,

adventitious root formation, lateral root initiation and subsequent outgrowth, and root hair elongation (Koltai, 2011, 2012; Ruyter-Spira *et al*., 2011; Rasmussen *et al*., 2012). Moreover, a broad range of developmental roles was postulated for SLs in the alleviation of secondary seed dormancy induced by high temperature (Toh *et al*., 2012), hypocotyl elongation (Hu *et al*., 2010; Tsuchiya *et al*., 2010), secondary growth (Agusti *et al*., 2011), light harvesting (Mayzlish-Gati *et al*., 2010; Tsuchiya *et al*., 2010), reproductive development (Snowden *et al*., 2005; Kohlen *et al*., 2012), and leaf senescence (Snowden *et al*., 2005; Ledger *et al*., 2010). SLs seem to be specifically involved in the establishment of the symbiosis with nitrogen-fixing bacteria in legumes, namely in the formation of indeterminate nodules (Soto *et al*., 2010; Foo and Davies, 2011; Foo *et al*., 2013). Finally, besides their hormonal role, SLs exuded into the rhizosphere stimulate the germination of parasitic plants (Yoneyama *et al*., 2010; Lechat *et al*., 2012) and the branching of arbuscular mycorrhizal fungi (AMF) (Akiyama *et al*., 2005; Bouwmeester *et al*., 2007; Yoshida *et al*., 2012). A recent report suggests that the hormonal effect on the elongation of rhizoids (the equivalent of root hairs in higher plants) in ancestral species of the green lineage pre-dates the exogenous function as signalling molecules in the rhizosphere (Delaux *et al*., 2012).

SLs are a family of carotenoid-derived terpenoid lactones mostly produced in roots (Matusova *et al*., 2005). The precursor all-*trans*-β-carotene is converted by the recently characterized β-carotene isomerase D27 into 9-*cis*-β-carotene (Alder *et al*., 2012). The isomerized substrate is then cleaved by two double bond-specific cleavage enzymes (carotenoid cleavage dioxygenases, CCDs), CCD7 and CCD8. The 9', 10' bond of 9-*cis*-β-carotene is cleaved by CCD7, yielding β-ionone (C_{13}) and 10'-apo-β-carotenal (C_{27}). The latter compound is subsequently cleaved and cyclized by CCD8 into a bioactive SL precursor named carlactone (Booker *et al*., 2004; Schwartz *et al*., 2004; Alder *et al*., 2012). Several orthologues of these two CCDs have been characterized in *Arabidopsis*, pea, petunia, rice, and tomato (Morris *et al*., 2001; Sorefan *et al*., 2003; Booker *et al*., 2004; Snowden *et al*., 2005; Zou *et al*., 2006; Arite *et al*., 2007; Drummond *et al*., 2009; Vogel *et al*., 2010; Kohlen *et al*., 2012). CCD8 orthologues are also characterized in kiwifruit, chrysanthemum, maize, and the moss *Physcomitrella patens* (Ledger *et al*., 2010; Liang *et al*., 2010; Proust *et al*., 2011; Guan *et al*., 2012). MAX1, a class-III cytochrome P450 protein of *Arabidopsis*, has also been proposed to act in the SL biosynthetic pathway, namely converting carlactone into 5-deoxystrigol, but its biochemical action still needs to be resolved experimentally (Booker *et al*., 2005; Alder *et al*., 2012). Other genes putatively involved in SL biosynthesis have been identified in several species (*SlORT1* and *AtPPD5*), but their exact function is so far unknown (Koltai *et al*., 2010*b*; Roose *et al*., 2011). No orthologues of any of the above biosynthetic genes have been characterized in *Lotus japonicus* yet.

Lotus japonicus is a perennial legume of temperate climates, and a model plant for several developmental processes and interactions with soil (micro)organisms (Handberg and Stougaard, 1992; Lohar and Bird, 2003); the first SL molecule described as a branching factor for AMF, 5-deoxystrigol, was isolated from this plant (Akiyama *et al*., 2005). Additionally, *L. japonicus* has a phyllotaxis distinct from that of other model plants such as *Arabidopsis*, pea, petunia, tomato, and rice. In fact, all of its cotyledonary axillary buds develop immediately into lateral shoots even in very young seedlings. This, and the regular, proliferative accessory (axillary) meristem initiation and immediate development of axillary shoots, makes *L. japonicus* an attractive experimental model to study the regulation of accessory meristem initiation and development (Alvarez *et al*., 2006). Namely, how SLs specifically affect the architecture of a plant with this kind of phyllotaxis is not known at present. Also, *L. japonicus* develops determinate nodules, differently from pea and *Medicago sativa*, the two species investigated so far for the role of SLs in nodulation.

In this study, the cloning of the *Lotus* orthologue of *CCD7* (*LjCCD7*), and an overall characterization of its role in the regulation of plant architecture, reproductive development, senescence, and root symbiosis are reported. The results also link *CCD7* expression with the regulation of determinate nodulation, reproduction, and senescence in *L. japonicus*. These latter phenotypes have not been reported so far for any *CCD7* orthologue.

Materials and methods

RNA isolation, cDNA synthesis, and quantitative reverse transcription–PCR (RT–qPCR)

For transcript quantification and rapid amplification of cDNA ends (RACE) cloning purposes, RNA was isolated from freshly harvested tissues of wild-type *L. japonicus* ecotype Gifu B-129 and transgenic lines in the same background with Tripure reagent (Roche). On-column DNase digestion was performed with an RNase-free DNase kit, and total RNA was further purified by an RNeasy Plant Mini Kit (both Qiagen). RNA quality and integrity were checked by NanoDrop ND-2000 and standard gel electrophoresis. A 1 µg aliquot of total RNA was reverse transcribed to cDNA with an iScript cDNA synthesis kit (Bio-Rad). RT–qPCRs were set up in 20 µl using the iQ SYBR Green Supermix on the iQ5 Real-Time PCR system (Bio-Rad). *LjCCD7*-specific primers are listed in Supplementary Table S1 available at *JXB* online. Ubiquitin (*LjUBI*) transcript was used as a normalizer (Yokota *et al*., 2009). Quantification followed the $2^{-\Delta\Delta Ct}$ method.

5'- and 3'-RACE

The putative *LjCCD7* gene was identified based on the EST (expressed sequence tag) in the Kazusa database (http://www.kazusa.or.jp/lotus/) aligning best under BlastP default settings with query sequences from *Arabidopsis* (GI: 330255400) and pea (GI: 90019042). The SMART RACE cDNA amplification kit (Clontech) was used to amplify the unknown ends of the coding sequence in a cDNA pool from *Lotus* roots, and cloning was performed using the Advantage 2 PCR enzyme system (Clontech) and primers UPM with GSP1 or GSP2 (Supplementary Table S1 at *JXB* online). PCR conditions for both cDNA ends were five cycles at 94 °C for 30 s, 72 °C for 3 min; five cycles at 94 °C for 30 s, 70 °C for 30 s, 72 °C for 3 min; and 25 cycles at 94 °C for 30 s, 68 °C for 30 s, and 72 °C for 3 min. RACE products were electrophoresed, tested with primers NestF and NestR (Supplementary Table S1 at *JXB* online), cloned in the pGEM-T easy vector (Promega), and sequenced (BMR

Genomics, Padova). The full-length sequence of *LjCCD7* (1866 bp) was assembled virtually with the Vector NTI Advance 11.0 and amplified from the aforementioned cDNA batch with primers LDF and LDR (Supplementary Table S1 at *JXB* online). The PCR product was cloned into pGEM-T to generate pGEM-T_LjCCD7, and sequenced. The resulting coding sequence is deposited in GenBank (ID: GU441766).

Plasmid constructs

For expression in *Escherichia coli* of glutathione *S*-transferase (GST)–LjCCD7, an *Eco*RI fragment was subcloned from pGEM-T_LjCCD7 into pGEX-5X-3. To generate the *LjCCD7* silencing vector, a 250 bp region (from 1451 bp downstream of the transcription start site to the stop codon, within the last exon) was amplified with *Pfu* polymerase (Promega) and primers RNAiF and RNAiR (Supplementary Table S1 at *JXB* online). The PCR product was directly sequenced and cloned in pDONR221 to generate the entry clone pDONR_LjCCD7. Finally, a single-step Gateway-based reaction was performed with pDONR_LjCCD7 and the destination vector pTKO2 (Snowden *et al*., 2005). In parallel, the negative control (NC) construct pTKO2_pENTR was generated with the empty entry vector pENTR4 and the destination vector pTKO2. Both pTKO2_LjCCD7 and pTKO2_pENTR constructs were sequenced with primer pairs 572F/1133R and 1388F/1847R (Supplementary Table S1 at *JXB* online).

Protein expression and in vitro enzyme assays

Cultures of *E. coli* BL21 (600 ml) harbouring pGEX_LjCCD7 or the empty vector in 2× YT medium (per litre: 16 g of tryptone, 10 g of yeast extract, and 5 g of NaCl) were grown at 28 °C until A_{600}=0.5. Recombinant protein expression was induced by 0.2 mM isopropyl-β-D-1-thiogalactopyranoside at 18 °C for 24 h. *Escherichia coli* cells were harvested by centrifugation at 4 °C, resuspended in cold STE buffer (100 mM NaCl, 10 mM TRIS, 1 mM EDTA, pH 8.0) containing 100 μg ml^{-1} lysozyme, incubated on ice for 15 min, and then lysed by sonication. The recombinant protein was purified with glutathione–Sepharose 4B (GE Healthcare), visualized by 10% SDS–PAGE, and electrotransferred to a blotting membrane (Fluorotrans, Fluka). Western blot analysis was performed by blocking with 5% non-fat dehydrated milk in TBST buffer (10 mM TRIS-HCl, 150 mM NaCl, and 0.05% Tween-20), followed by incubation with polyclonal antibodies against GST and then against alkaline phosphatase (Sigma) diluted respectively at 1:5000 and 1:10 000 in TBST buffer with 0.5% milk. Extensive washing in TBST buffer was followed by nitroblue tetrazolium and 5-bromo-4-chloro-3-indolyl-phosphate staining (Sigma).

For *in vitro* enzymatic assays, reactions were performed as previously reported (Schwartz *et al*., 2004; Marasco *et al*., 2006) with minor modifications. Soluble proteins were quantified with the Bradford reagent (Bio-Rad). Aliquots of the affinity-purified GST–LjCCD7 protein (50–100 μg in 100 μl of glutathione elution buffer) were brought to 400 μl with 100 mM TRIS buffer, pH 7.0 containing 300 mM NaCl, 0.5 mM $FeSO_4$, 10 mM dithiothreitol (DTT), 5 mM ascorbate, and 0.05% Triton X-100. After 20 min of equilibration, 80 μl of substrate (0.5 mM Type II β-carotene in acetonitrile; presumably all-*trans*, Sigma C4582) were added. Note that even if 9-*cis*-β-carotene is the real substrate of CCD7 (Alder *et al*., 2012), *trans*-β-carotene can also be cleaved (though not as efficiently), and is the commercially available isomer. Reaction tubes were gently shaken in the dark at 28 °C for 5 h before being quenched with 50 μl of 33% formaldehyde for 10 min at 37 °C. A 600 μl aliquot of acetonitrile was added to each tube and the organic layer was saved for HPLC analysis. A Perkin Elmer series 200 HPLC system equipped with a diode array was used for detection. Separation was performed using a C18 reversed-phase column (250 mm×4.6 mm internal diameter, 5 μm particles; YMC Europe) with the solvent system methanol:water (70:30, v/v) containing 0.1% ammonium acetate (B) and methanol (A) as described (Marasco *et al*., 2006).

Plant transformation and regeneration

The transformation of *L. japonicus* ecotype Gifu B-129 was performed via *Agrobacterium tumefaciens* strain EHA105 harbouring pTKO2_LjCCD7 or pTKO2_pENTR (NC) as detailed previously (Barbulova *et al*., 2005) with slight changes. Briefly, roots, shoots, and leaves were excised from 3-week-old seedlings grown in Petri dishes on Gamborg B5 (Sigma) and separately conditioned onto callus-inducing medium (CIM) (Lombari *et al*., 2003) for an additional week. Segments were dipped for 25 min into *A. tumefaciens* cultures grown to A_{600}=0.4–0.6 at 28 °C in YEB medium (per litre: 5 g of peptone, 5 g of beef extract, 1 g of yeast extract, 5 g of sucrose, and 0.5 g of $MgCl_2$). The explants were then dried quickly on sterile filter paper and transferred onto fresh CIM plates. After 3 d of co-cultivation in the dark, bacterial slime was rinsed away in sterile water. Explants were dried on sterile filter paper and transferred on CIM plus 500 mg l^{-1} cefotaxime and 200 mg l^{-1} carbenicillin. After 2 d, transformed explants were selected on CIM plus 500 mg l^{-1} cefotaxime, 200 mg l^{-1} carbenicillin, and 100 mg l^{-1} kanamycin. After 3–4 weeks, the kanamycin-resistant sectors were transferred on shoot-inducing medium (SIM) (Barbulova *et al*., 2005) containing 500 mg l^{-1} cefotaxime, 100 mg l^{-1} kanamycin, and 0.5 mg l^{-1} thidiazuron. After 2 weeks, calli from which rudimentary shoots were emerging were transferred on SIM plus 500 mg l^{-1} cefotaxime, 100 mg l^{-1} kanamycin, and 0.05 mg l^{-1} thidiazuron for shoot elongation. Regenerated T_0 plants with 1.5–2.0 cm roots were transferred into pots filled with 2:1 perlite:*Arabidopsis* special soil (Horticoop) for seed setting. Their seeds (T_1 generation) were surface-sterilized (70% ethanol for 1 min and 2.5% NaClO for 25 min), stratified at 4 °C for 2–3 d on jellified Gamborg B5, then germinated at 24 °C in a growth chamber (16 h light/8 h dark). Then they were transferred in perlite-filled pots in a growth chamber (20–21 °C, 16 h light/8 h dark); 3-week-old seedlings from >40 independent T_0 transgenic lines were screened by PCR with primer pairs KanF/KanR and RNAiR1/pTKO2-1847R (Supplementary Table S1 at *JXB* online) for the integration of the transgenic cassette. Among those with an SL-related phenotype, lines PG, P9, and P16 were selected for further studies because of their obvious shoot phenotype and homogeneous degree of target gene silencing and SL depletion. At the T_0 generation, these were hemizygous (as ascertained by PCR screening of the T_1 progeny obtained from self-pollination). Homozygous T_1 individuals were retained on the basis of progeny segregation analysis and propagated to T_2 and T_3. All plants included in all experiments were tested for cassette integration and *LjCCD7* transcript levels in roots (if possible), and showed an obvious shoot phenotype.

Plant phenotyping

Seedlings of the wild type and RNA interference (RNAi) line P16 (unless otherwise stated) were used for metabolic (T_1 generation) and phenotypic analysis (T_0, T_1, T_2, and/or T_3 generations, depending on the phenotypic character; for details, see the figure legends). Wild-type and/or transgenic NC plants were used interchangeably as controls, since no differences in *LjCCD7* expression, SL content, or general morphology were recorded. Surface-sterilized seeds were pre-conditioned on wet filter paper for 2 d, and then moved into a growth chamber (16 h light/8 h dark, 24 °C). Two-week-old seedlings were grown in 18 cm diameter pots filled with *Arabidopsis* special soil and perlite (1:2) in a greenhouse (16 h light/8 h dark, 20 °C), watered daily, and given 'Hornum' nutrients (Handberg and Stougaard, 1992) twice per week. Different traits were evaluated at different plant ages, as indicated in the Results.

For all statistical analyses on shoot branching, only branches longer than 0.5 cm were included. Root parameters (total length, area, and volume) were calculated by the WinRhizo software on digital images of whole apparatuses. For primary root length and stem width measurements, organs were photographed and analysed by ImageJ software. For chlorophyll quantification, two compound leaves, located at the same position on the main stem, were collected from three individual plants for each of the RNAi lines (PG, P9,

and P16) and analysed as reported (Ni *et al*., 2009). From the third round of seed setting until plants were 11 months old, flowers were counted on three plants for each of the three RNAi lines and NCs, and pods were harvested. The definitions used to describe *Lotus* phyllotaxis are as in Alvarez *et al*. (2006).

SL extraction and LC-MS/MS analysis

Two-week-old seedlings of transgenic line P16 and transgenic NC (15 each) were transplanted into an X-stream 20 aeroponic system (Nutriculture) and supplied with 5 litres of modified half-strength Hoagland solution (Hoagland and Arnon, 1950) refreshed twice a week. Experiments were performed 3–4 weeks later, when roots were fully developed but before the emergence of flowers. Root exudates were collected, purified, and concentrated as described previously (Liu *et al*., 2011). One day before exudate collection, roots were thoroughly rinsed with distilled water and the nutrient solution was refreshed to eliminate accumulated SLs. After exudate collection, roots from five plants for each sample were pooled and stored at –80 °C for later use. The experiment was repeated three times.

SL extraction from root exudates and tissues was performed as previously reported (López-Ráez *et al*., 2010) with minor modifications. Exudates were firstly condensed into 50 ml 60% acetone fractions eluted from a C18 column (GracePure 5000 mg 20 ml^{-1}), of which 2 ml fractions were used, and each mixed with 200 µl of 0.1 nmol ml^{-1} $[^2H]_6$-5-deoxystrigol in acetone as internal standard for further purification. Once samples were well evaporated under a speed vacuum, the residues were dissolved in 50 µl of ethyl acetate and diluted with 4 ml of hexane for silica column purification (GracePure 200 mg 3 ml^{-1}). Elutions of 40% or 60% ethyl acetate in hexane were combined and dried. The residues were dissolved in 200 µl of acetonitrile:water (25:75), filtered, and used for ultraperformance liquid chromatography tandem spectrometry (UPLC-MS/MS) analysis. Fresh frozen root samples (0.5 g each) were ground and extracted with 2 ml of 0.05 nmol ml^{-1} $[^2H]_6$-5-deoxystrigol, used as internal standard, in ethyl acetate. The samples were sonicated for 15 min in a Branson 3510 ultrasonic bath (Branson Ultrasonics, USA). Samples were centrifuged for 15 min at 2500 *g*; the supernatant was gently transferred to 4 ml glass vials, and the pellet was re-extracted with 2 ml of ethyl acetate without internal standard. Supernatants were combined, and ethyl acetate evaporated under vacuum. The following steps were performed as described above in root exudate purification. A Xevo tandem mass spectrometer (Waters) equipped with an electrospray ionization (ESI) source and coupled to an Acquity UPLC system (Waters) was used for SL detection and identification as described (Kohlen *et al*., 2012). Data were analysed with MassLynx 4.1 (Waters).

Rhizobia and AMF infection assays

Mesorhizobium loti strain R7A was used for nodulation assays. Slightly lignified shoots were cut off 4-month-old plants (line P16), and set for root induction in rockwool. When roots were ~0.5–1.0 cm long (1.5–2.0 weeks), plants were transferred to perlite for another week, and irrigated with B&D nutrient solution (Broughton and Dilworth, 1971). Each plant was inoculated with 30 ml of bacterial culture grown at 28 °C in YMB medium (per litre: 0.4 g of yeast extract, 10.0 g of mannitol, 5.0 g of K_2HPO_4, 0.2 g of $MgSO_4$, 0.1 g of NaCl, 0.5 g of sucrose) and diluted to a final A_{600} of ~0.05. Nodules and lateral roots were counted 2 weeks post-inoculation.

AMF colonization assessment was carried out on plants infected with *Gigaspora margarita* spores in 'Millipore sandwiches' (Novero *et al*., 2002). Briefly, seeds sterilized with sulphuric acid were pregerminated on 0.6% water agar. Roots were placed between two nitrocellulose membranes (5 cm diameter, 0.45 µm pores; Millipore) with 20 fungal spores sterilized by chloramine T (3%) and streptomycin sulphate (0.3%). After 4 weeks of co-culture, roots were sampled and stained with cotton blue (0.1% in lactic acid) to visualize fungal structures. For each genotype, intraradical colonization was evaluated in three plants and at least 160 cm of roots under an optical microscope (Trouvelot *et al*., 1986).

Statistical analysis

One-way analysis of variance (ANOVA) was performed on all data sets by using GenStat for Windows. If needed, data were also subjected to Student's *t*-test.

Results

Cloning of LjCCD7 and in vitro confirmation of its enzymatic activity

MAX3 from *Arabidopsis* and RMS5 from pea were used to interrogate the EST and genomic database at the Kazusa DNA Research Institute. The EST aligning best to the queries (LjSGA_131670.1, 873 bp) was assumed to derive from their *bona fide Lotus* orthologue, designated *LjCCD7*. Based on the partial coding sequence available, the missing cDNA ends of *LjCCD7* were obtained by 5'- and 3'-RACE followed by direct amplification of the full-length coding sequence. The predicted polypeptide was 74% identical to RMS5 and 58% identical to MAX3. A phylogenetic tree (Supplementary Fig. S1 at *JXB* online) was produced from an alignment of several CCD7 homologues from land plants and moss, as well as of some putative homologues identified in cyanobacteria (Cui *et al*., 2012). The CCD7 proteins clustered into several clades, with LjCCD7 in the subclade of predicted leguminous homologues within the dicot clade, as expected (Supplementary Fig. S1 at *JXB* online).

To verify whether the phylogenetic prediction corresponded to a conserved enzymatic function, the carotenoid cleavage activity of LjCCD7 was tested *in vitro*. To do so, recombinant GST–LjCCD7 was affinity purified from *E. coli* cells, and its apparent size (~98 kDa) checked by SDS–PAGE and western blotting (Supplementary Fig. S2A, B at *JXB* online). After 5 h incubation in the presence of β-carotene (C_{40}) as substrate, two compounds were detected in the presence of GST–LjCCD7 and not with GST alone. One of them had a visible spectrum peak and retention time similar to β-ionone (C_{13}; Supplementary Fig. S2C). The second was deduced to be 10'-apo-β-carotenal (Supplementary Fig. S2D); that is, the complementary C_{27} that would result from the cleavage of the 9', 10'-bond of β-carotene by CCD7. These results agreed with previous work in *Arabidopsis* and tomato (Booker *et al*., 2004; Schwartz *et al*., 2004; Vogel *et al*., 2010) and proved that the cloned cDNA corresponds to a protein endowed with carotenoid cleavage activity *in vitro*. With the outcome of phylogenetic analysis shown in Supplementary Fig. S1, they support the notion that the identified gene encodes the *L. japonicus* CCD7 orthologue.

To study the expression pattern of *LjCCD7*, RT–qPCR was performed on RNA samples from a range of vegetative tissues from 8-week-old wild-type plants. As in *Arabidopsis* (Booker *et al*., 2004), pea (Johnson *et al*., 2006), petunia (Drummond *et al*., 2009), and tomato (Vogel *et al*., 2010), *LjCCD7* was predominantly expressed in roots, ~2-fold more than in leaves and the shoot apex. *LjCCD7* transcript was

also detected in stipules, although 13 times less abundantly than in roots (Fig. 1A).

Generation and molecular characterization of transgenic lines impaired in LjCCD7 expression

To elucidate the biological function of *LjCCD7 in planta*, >40 independent RNAi lines were generated. Three of them (PG, P9, and P16) displayed ~70% less *LjCCD7* transcript in roots relative to corresponding transgenic control plants (Fig. 1B), and were selected for further analysis. *CCD7* is a key biosynthetic gene for SLs, so the presence of all known SLs in the root exudates and extracts of wild-type *Lotus* was initially checked (not shown); 5-deoxystrigol was the only one detected, in accordance with previous work (Sugimoto and Ueyama, 2008). 5-Deoxystrigol was therefore quantified in both root exudates and extracts of wild-type *L. japonicus* and transgenic seedlings (line P16). In all samples, one distinct peak was detected that had the retention time and transitions corresponding to 5-deoxystrigol. 5-Deoxystrigol levels were higher in root exudates than in root extracts, both in wild-type seedlings and in the *CCD7*-silenced line. Metabolite abundance in RNAi plants was decreased by 81% and 73% in root exudates and extracts, respectively, relative to the non-silenced control seedlings (Fig. 1C).

Decreased LjCCD7 transcript correlates with changes in shoot and root morphology

Since SLs regulate plant architecture, experiments were conducted to assess whether the reduction in *LjCCD7* transcript and SL content was associated with altered morphology in RNAi line P16; lines P9 and PG, in which *LjCCD7* was silenced comparably, were also evaluated. From 3 weeks after germination, the RNAi lines exhibited a clearly stunted and bushy phenotype (Fig. 2A). Shoot branches were counted at two time points. Eight-week-old transgenic plants were significantly more branched than controls transformed with the empty vector: RNAi lines displayed 5.3, 2.1, and 4.0 times more cotyledonary, primary, and secondary aerial branches, respectively (Fig. 2B). When 6 months old, plants of the PG, P9, and P16 lines displayed 6.4, 6.6, and 5.7 times more total shoot branches relative to the controls, respectively (Fig. 2C). No branches of secondary or higher order occurred in the

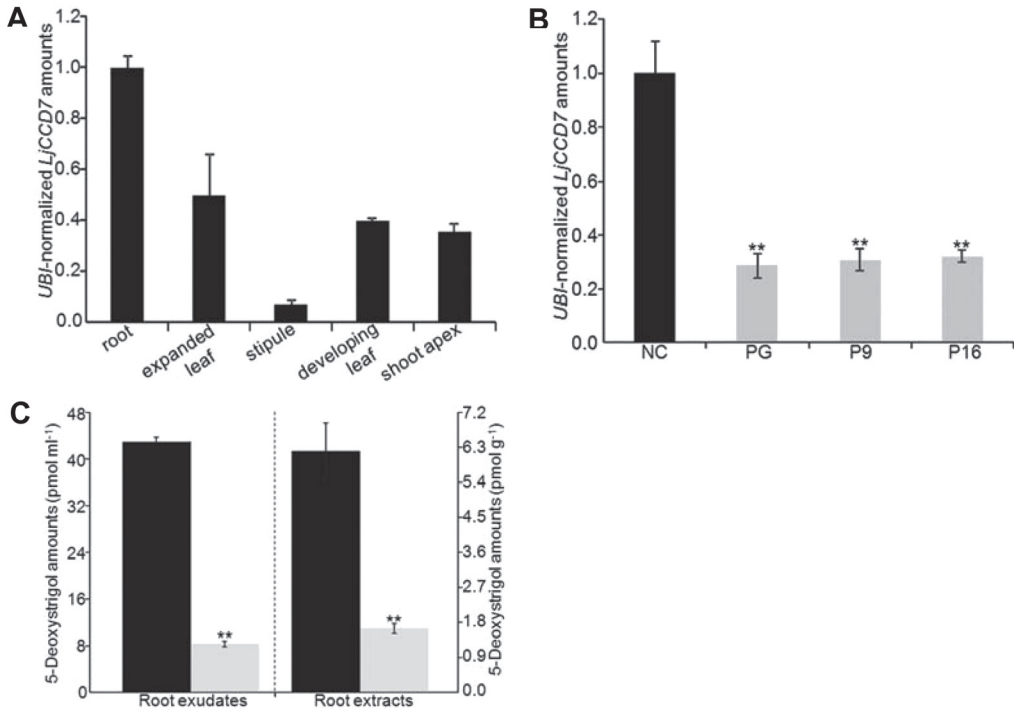

Fig. 1. *LjCCD7* transcription pattern, and molecular and metabolic characterization of *CCD7*-silenced lines. (A) *LjCCD7* transcript abundance in various vegetative tissues relative to root expression level in 8-week-old wild-type *L. japonicus*. Values are the average of *n* biological and three technical replicates ±SE, normalized to *LjUBI* transcript levels. *n*=6 for root and shoot apex, *n*=5 for expanded or developing leaf, *n*=4 for stipule. (B) Relative *LjCCD7* transcript amounts in roots of RNAi lines PG, P9, and P16 (grey bars), compared with a line transformed with the empty vector (negative control, NC; black bar). Values are normalized to *LjUBI* transcript amounts, and displayed as means of *n* biological and three technical replicates ±SE (*n*=3 for each RNAi line and n=5 for controls, all at the T_1 generation). The asterisks indicate statistically significant differences for $P < 0.01$. (C) LC-MS/MS analysis of 5-deoxystrigol content in root exudates and extracts of 6/7-week-old, aeroponically grown plants of the wild type (black bars) and of the *CCD7*-knockdown line P16 at generation T_1 (grey bars). Twenty-four hours before collection of root exudates, the nutrient solution was refreshed for 15 plants. In root extracts, three independent samples were used and each consisted of five plants. Error bars represent the SE for three analytical replicates. The asterisks indicate a statistically significant difference for $P < 0.01$.

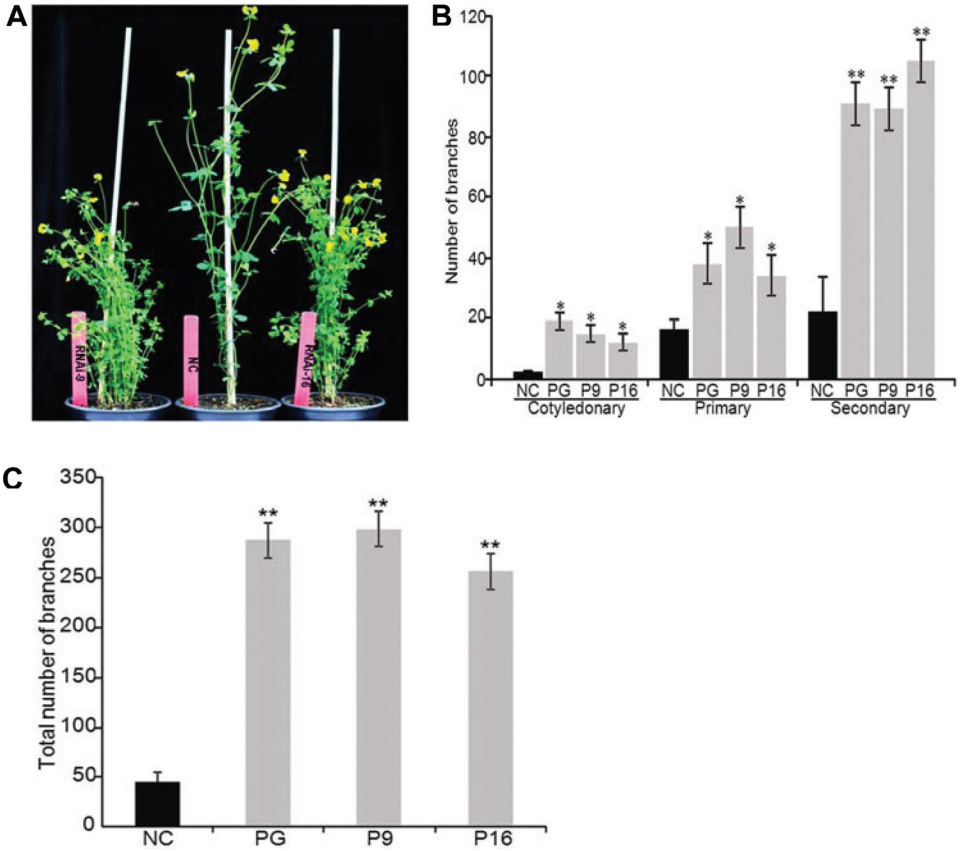

Fig. 2. Shoot architecture analysis of RNAi lines. (A) Representative comparison of shoot branching appearance of RNAi line P16 and negative controls (NCs) transformed with the empty vector, both 10 weeks old and at the T_1 generation. (B) Cotyledonary, primary, and secondary aerial branches of 8-week-old RNAi plants from lines PG, P9, and P16 (grey bars) and the NC (black bars). Each value represents the mean ±SD (n=4 and n=3 T_1 plants for control and each RNAi genotype, respectively). The asterisks indicate statistically significant differences for $^*P < 0.05$ and $^{**}P < 0.01$. (C) Total shoot branches of 6-month-old T_1 RNAi lines PG, P9, and P16 (grey bars) and the NC (black bar). Each value represents the mean ±SD (n=14 for control versus n=3 for each RNAi line). The asterisks indicate statistically significant differences for $P < 0.01$. (This figure is available in colour at *JXB* online.)

transgenic control plants at this or later stages, in contrast to RNAi lines (Supplementary Fig. S3A, B at *JXB* online). RNAi plants also had a significantly reduced main stem height (39, 40, and 29% shorter than the transgenic NC line, respectively; Fig. 3A). Reduced plant height was not due to a reduced number of nodes in the RNAi lines (not shown). Rather, internodes were significantly shorter in silenced plants compared with the corresponding control, particularly in high-order nodes. In fact, internodes IV–VII of the main stems were ~30–40% shorter in line P16 than in the wild type (Fig. 3B). The same was observed for most internodes above node III in secondary shoot branches (Fig. 3C). SLs have been shown to control the thickening of stems and roots (Agusti *et al*., 2011). As expected, RNAi line P16 displayed an ~39% reduction of secondary shoot diameter compared with the control (Fig. 3D, E).

SLs affect root development, including lateral root formation, and primary root and root hair development (Koltai, 2011; Ruyter-Spira *et al*., 2011). To assess the function of SLs in *Lotus* root development, plants of RNAi line P16 were grown either in aeroponic tanks or in pots. Under all conditions, the RNAi line consistently showed more lateral roots and longer primary roots (Fig. 4A). Five-week-old plants grown in aeroponic tanks were used for quantitative analysis: RNAi plants had a 1.6–2.0 times higher total root length, area, and volume than controls (Fig. 4B, C). Notably, the primary root of the RNAi line was significantly longer than in the corresponding controls grown either in the aeroponic system or in pots.

Effect of LjCCD7 silencing on reproduction

Lotus japonicus ecotype 'Gifu' flowers profusely and, in subsequent rounds, yields thousands of seeds within months after pollination (Handberg and Stougaard, 1992). We observed that seed production was severely impaired in RNAi plants compared with controls, particularly after two rounds of seed settings (representative individuals are shown in Supplementary Fig. S4A at *JXB* online). For a statistical assessment, all flowers from the third round on were counted and pods were harvested separately. An at least 7-fold reduction of flower and pod numbers was observed in RNAi lines relative to the NC (Fig. 5). After the above-ground part of 11-month-old plants was lopped off, ~40 times fewer pods

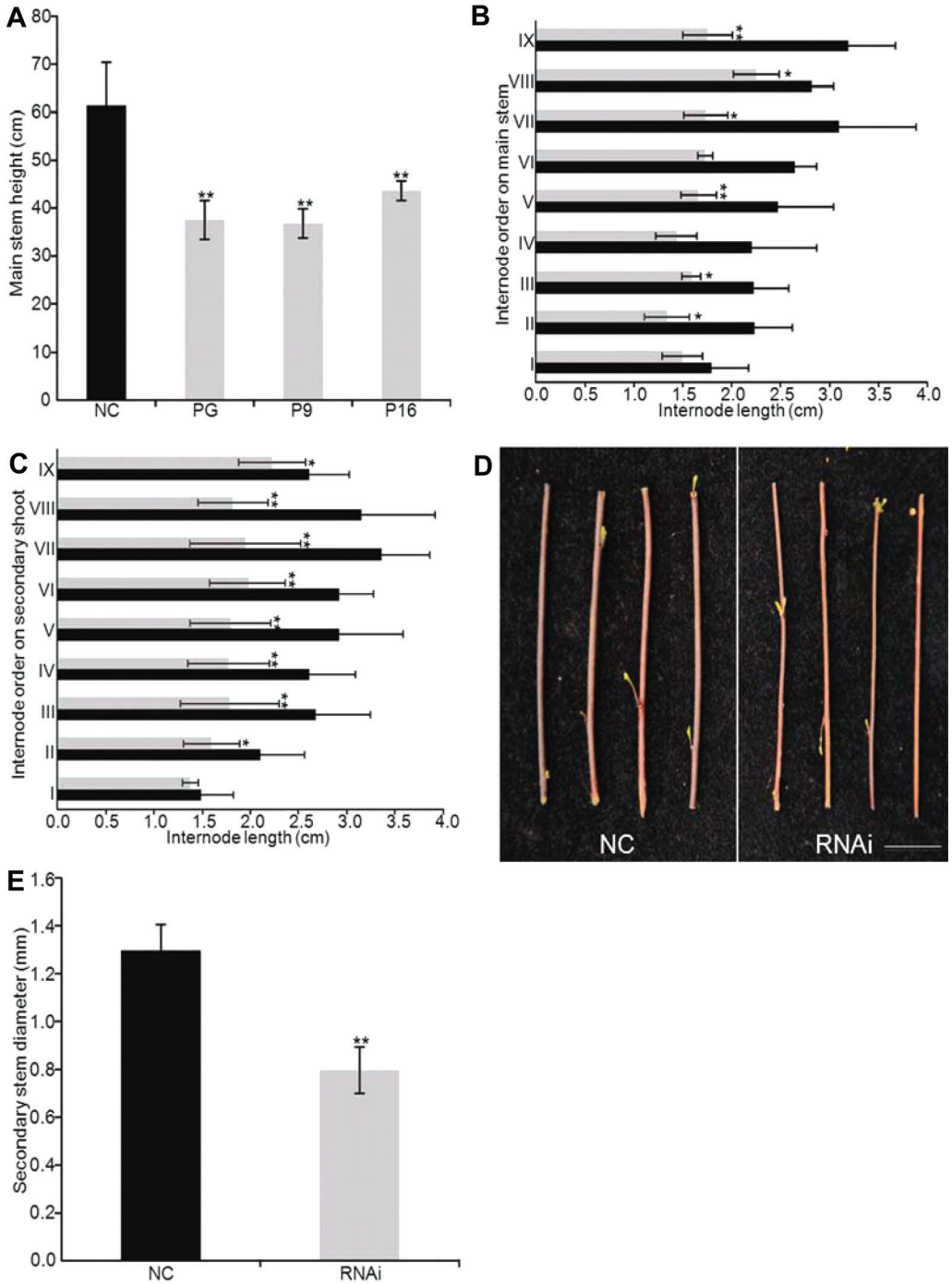

Fig. 3. Shoot morphology of SL-depleted versus control plants. (A) Plant height of 6-month-old T_1 transgenic negative control (NC, black bar) and RNAi lines PG, P9, and P16 (grey bars). Error bars represent the SD of the means (n = 10 and n=3 for NC and each RNAi line, respectively). Asterisks indicate statistically significant differences between each RNAi line and the NC, for $P < 0.01$. (B and C) Comparison of internode length between 2.5-month-old wild-type plants (black bars) and RNAi line P16, T_1 generation (grey bars). The internode above the cotyledons was set as the first node in the acropetal direction, so internode I lies between collar and cotyledonary node I, and so forth. Both the internodes from the main stem (B) and basal secondary shoots (C) were used for analysis. Data are means ±SD ($n \geq 6$). Asterisks indicate statistically significant differences for $^*P < 0.05$ and $^{**}P < 0.01$. (D) Representative display of secondary stem width in SL-depleted (RNAi) and NC plants. The picture was taken on 3-month-old T_1 plants of RNAi line P16 and transgenic plants transformed with the empty vector. Bar scale=1 cm. (E) Quantification of secondary stem width. Data were obtained on 3-month-old T_1 plants and are presented as means ±SD (n=22 for NC, black bar; and n=45 for RNAi line P16, grey bar). The asterisks indicate significantly different values for $P < 0.01$. (This figure is available in colour at *JXB* online.)

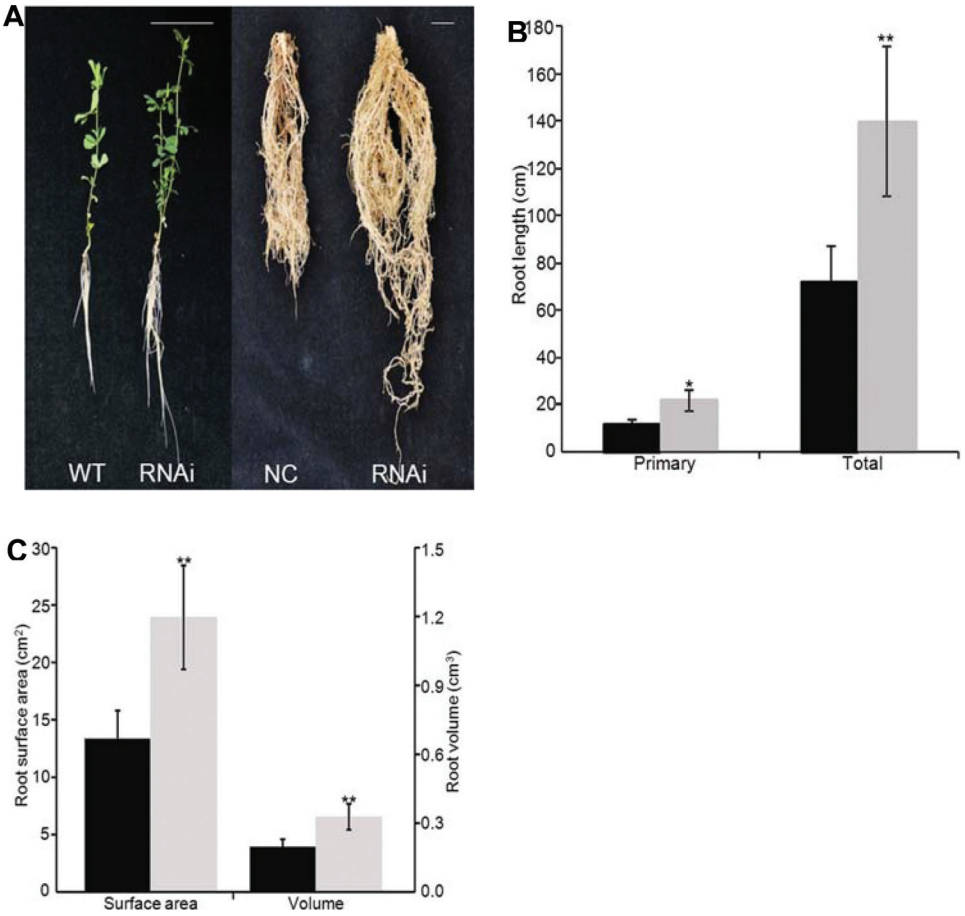

Fig. 4. Phenotypic characterization of roots in SL-depleted and control plants. (A) Root morphology of 4-week-old plants representative of the wild type and RNAi line P16, T_1 generation (left panel). The plants in the picture were grown for 1 week in Petri dishes in a growth chamber, 1 week in perlite, and another 2 weeks in aeroponic tanks. Root shape of 3.5-month-old transgenic negative control (NC) and RNAi line P16, T_2 generation (right panel), cultivated in pots filled with *Arabidopsis* soil (Horticoop) and perlite (1:2). (B and C) Quantification of root parameters in 5-week-old wild-type (black bars) and RNAi plants (line P16 at T_1 generation, grey bars). Data are presented as means ±SD ($n > 6$). Asterisks indicate statistically significant differences for $^*P < 0.05$ and $^{**}P < 0.01$. (This figure is available in colour at *JXB* online.)

were counted on the emergent branches of RNAi plants than on controls (not shown). Impairment of flower and seed setting was less severe for line P16 than lines PG and P9, which is why the first was used for most analyses. There were no significant changes with respect to size, shape, or colour of the flowers, pods, and seeds. Given the intimate cross-talk occurring between SLs and auxin during reproductive development (Kohlen *et al*., 2012), the levels of free indole acetic acid (IAA) were measured in flowers collected at anthesis. Only a mild but statistically non-significant reduction was observed in RNAi line P16 compared with controls (Supplementary Fig. S4B at *JXB* online).

Effect of decreased LjCCD7 transcript levels on plant senescence

Lotus is a deciduous perennial displaying progressive leaf senescence and abscission in temperate climates. Since a role for SLs in senescence had been proposed (Snowden *et al*., 2005; Ledger *et al*., 2010), the leaves of the transgenic plants were monitored for any obvious colour change compared with control, and chlorophyll in leaves of comparable physiological age was quantified. All three RNAi lines remained green for a longer time than the control (see Supplementary Fig. S5A at *JXB* online) and accumulated significantly more chlorophyll *a* (Chl*a*) and Chl*b* than the NC, with a cumulative 2-fold increase in total chlorophyll content when ~8 months old (Fig. 6A). At a younger stage (~3 months old), RNAi lines PG and P9 showed a significant increase in Chl*a* and Chl*b*, respectively; however, total chlorophyll content was not significantly different from that of the NC (Fig. 6A). When the top and internal part of 8-month-old RNAi plants left to senesce spontaneously had slightly started to fade in colour, controls were already severely senescing throughout their aerial parts (Supplementary Fig. S5B at *JXB* online). Also, more new shoots and branches kept emerging in RNAi lines compared with NCls (Supplementary Fig. S3C at *JXB* online). Finally, the RNAi line had higher biomass relative to control plants when ~3.5 months old (Fig. 6B); the trend was maintained with plant ageing. However, the shoot-to-root ratio

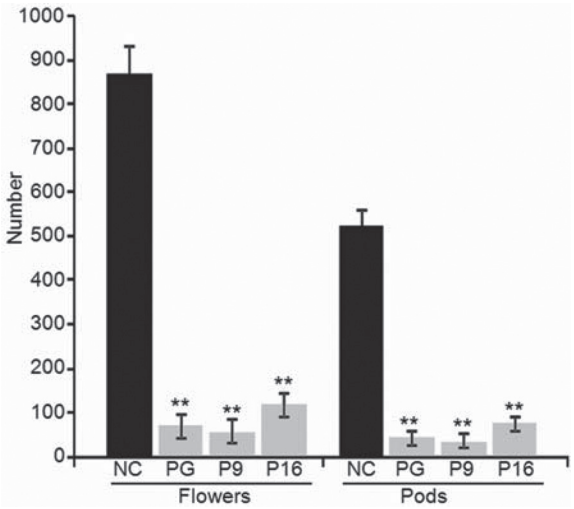

Fig. 5. *LjCCD7* transcript correlates with flower and pod number. Quantification of flowers and pods in 11-month-old transgenic negative control (NC, black bars) and RNAi lines PG, P9, and P16 at the T_1 generation (grey bars). Values are means ±SD (n=3 independent plants per genotype). The asterisks indicate statistically significant differences for $P < 0.01$.

was largely unchanged (average ratio ±SD: 2.796 ± 0.204 for RNAi lines versus 2.591 ± 0.094 for controls; data in Fig. 6B).

LjCCD7-silenced Lotus nodulates less but is colonized by AMF as much as control plants

The influence of SLs on *Lotus* determinate root nodules was explored. There were no significant differences in root fresh weight of RNAi plants compared with the wild-type and NC plants (not shown). However, their adventitious roots were significantly more branched also in the specific culture conditions used for this test (Fig. 7A, B). Although this situation potentially offers a larger surface to rhizobial infection for the same root biomass, RNAi roots carried significantly fewer nodules per gram of fresh weight than the NC 2 weeks post-inoculation (~20% reduction; Fig. 7C). In contrast, when controls and RNAi lines P16 and P9 were inoculated with spores of the AMF *G. margarita*, no significant differences in the colonization parameters evaluated were detected (Fig. 7D). SL-depleted roots supported both extra- and intraradical mycelium, which did not differ in quantity and developmental pattern from control roots. Also, arbuscules were morphologically indistinguishable (not shown).

Discussion

The role of SLs in the regulation of plant architecture is conserved in L. japonicus, but with some peculiarities

The phenotype of the SL-depleted *L. japonicus* plants characterized in this study was overall expected, on the basis of previously published work. RNAi plants were in fact stunted and their shoots more branched than controls, as were root apparatuses. More adventitious roots (not shown) were also observed, consistent with published data on *Arabidopsis* and pea (Rasmussen *et al.*, 2012). Notwithstanding, the shoot morphology of *L. japonicus* is quite different from that of other model plant species, which makes it an attractive model to study SL function. In fact, in wild-type *Lotus*, the axillary buds in the cotyledonary node or in the leaf axils are already visible during the early vegetative stage. Once these buds are initiated, they develop directly into lateral branches without being inhibited by any factors released by the shoot apical meristems. Thereafter, numerous accessory meristems will potentially develop lateral branches in the cotyledonary node zone, but in the aerial part only a single bud in the leaf axis develops into a branch while the others remain dormant (Alvarez *et al.*, 2006). This peculiar developmental pattern was reflected

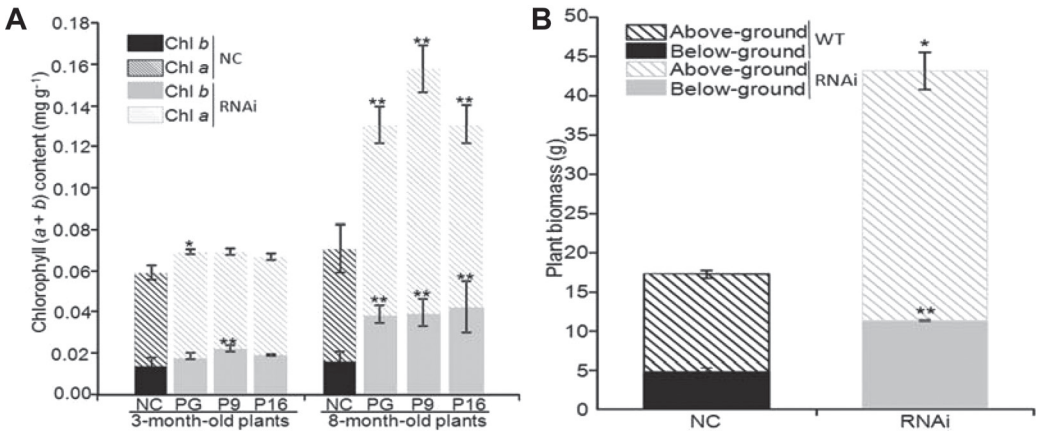

Fig. 6. *LjCCD7* influences age-related senescence progression and biomass in *Lotus*. (A) Total chlorophyll (Chl*a*, striped bars; Chl*b*, solid bars) in leaves of transgenic negative controls (NC, black bars) and RNAi lines PG, P9, and P16 at the T_1 generation (grey bars), 3 or 8 months old. Values are means ±SD (n=8 for each RNAi line and n=7 for NC). The asterisks indicate significant differences of Chl*a* and Chl*b* between RNAi plants and NCs of the same age for $^*P < 0.05$ and $^{**}P < 0.01$. (B) Fresh weight of roots and aerial parts in 3.5-month-old wild-type plants (black bars) compared with RNAi line P16, T_1 generation (grey bars). Values are means ±SD ($n \geq 6$). The asterisks indicate statistically significant differences for $^*P < 0.05$ and $^{**}P < 0.01$.

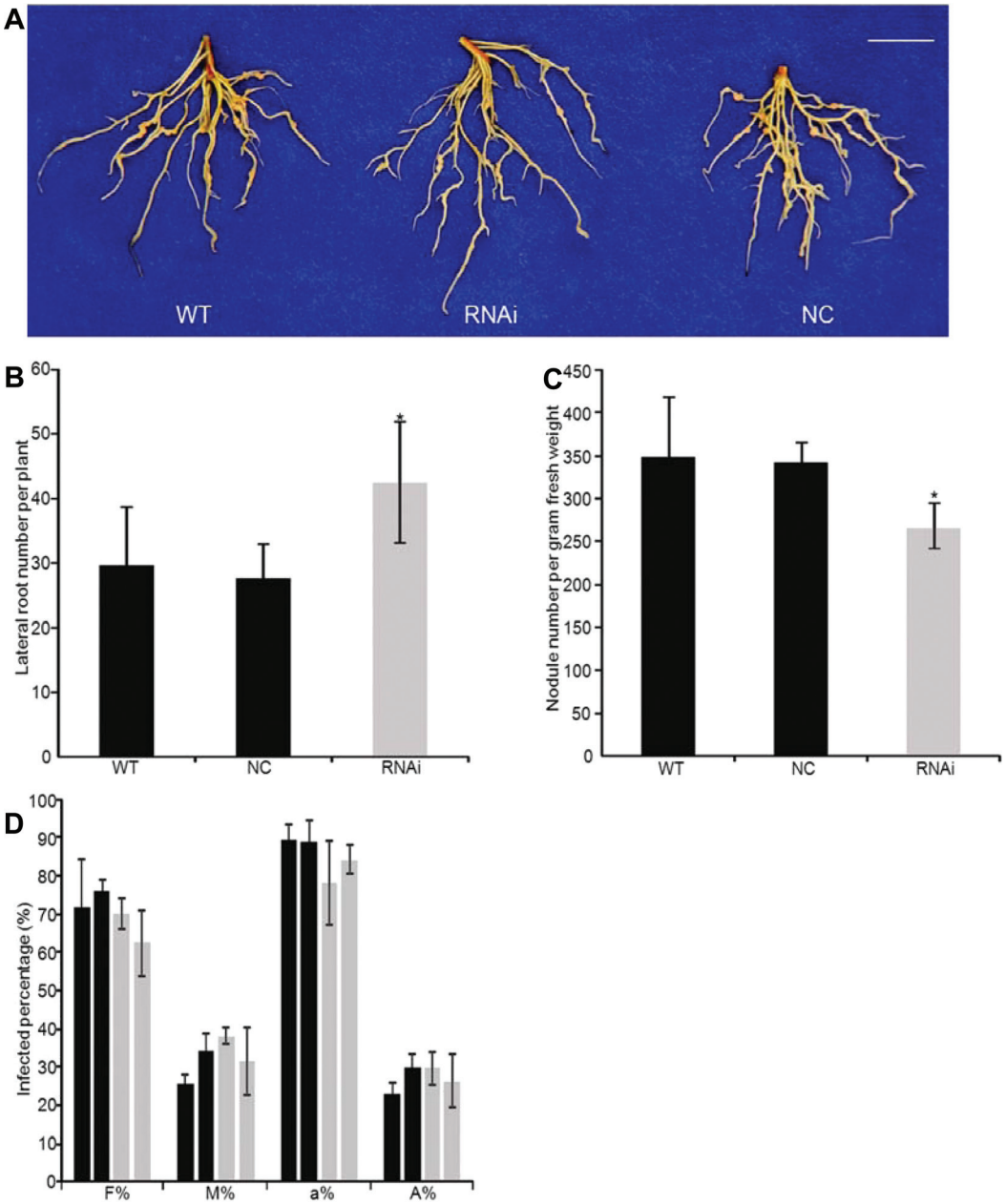

Fig. 7. SL-depleted *Lotus* plants nodulate less than controls but are not affected in AM symbiosis. (A) Representative picture of the differences in nodule number and root development detected between the wild type (left), RNAi line P16 (middle), and the transgenic negative control (NC, right), T_1 generation, 2 weeks after inoculation in perlite. (B) Root branching and (C) nodule number per gram of fresh root weight of 4-week-old roots in the wild type and NCs (black bars), and RNAi line P16, T_1 generation (grey bar). All values are displayed as means ±SD (n=17 for the wild type, n=6 for NC, and n=14 for the RNAi line). Asterisks indicate significant differences for $^*P < 0.05$. (D) Results of mycorrhization tests on controls (wild-type and NC plants, black bars) and RNAi lines P9 and P16, T_2 generation (grey bars). Trouvelot tests were performed on n=3 root apparatuses for each genotype, sandwich-inoculated with *Gigaspora margarita* spores. F%, frequency of mycorrhization; M%, intensity of mycorrhization; a%, percentage of arbuscules within the infected areas. A%, percentage of arbuscules in the whole root system. (This figure is available in colour at *JXB* online.)

in some specific shoot features in the SL-depleted plants. In contrast to most SL-related phenotypes described so far, in fact, branching of secondary shoots was highly increased compared with controls. This phenotype has been reported, though to a milder extent, only in *CCD7*- and *CCD8*-silenced tomato plants (Vogel *et al*., 2010; Kohlen *et al*., 2012). In transgenic Lotus, this increase was most probably due to several of the accessory buds in the aerial axils developing into lateral shoots, in contrast to what happens in the wild type (Alvarez *et al*., 2006). Also, many more basal branches than in the wild type were produced from the activity of accessory buds in the cotyledonary axil, resulting in more numerous primary shoots (Supplementary Fig. S3C at *JXB* online). Primary and secondary shoots were shorter in *CCD7*-silenced

plants compared with control plants because of a reduced internode length (as in petunia and maize) (Snowden *et al*., 2005; Guan *et al*., 2012) rather than number (as in tomato) (Kohlen *et al*., 2012).

LjCCD7-silenced plants differed slightly but significantly from other published SL mutants at the root level as well, in that they consistently exhibited longer primary roots than the controls. Results in *Arabidopsis*, rice, and maize point instead to a role for SLs in the promotion of primary root growth (Koltai *et al*., 2010*a*; Ruyter-Spira *et al*., 2011; Arite *et al*., 2012; Guan *et al*., 2012). In these species, SLs were proposed to alter the auxin gradient in the root tips, thus changing both the number and length of the cells located in the meristem and transition zone of primary roots. The results suggest that the role of SLs in primary root development differs from species to species, possibly in relation to varying endogenous hormonal levels.

Finally, the above- and below-ground mass of SL-depleted plants was increased, so that the shoot-to-root biomass ratio was comparable with that of controls. This observation differs from what has been reported for the petunia *ccd7*/*dad3* mutant, which displays a higher shoot-to-root ratio than the wild type (Snowden *et al*., 2005). This discrepancy may be due to the different species, growth conditions (hydroponic for petunia), and/or physiological age of the plants.

CCD7 affects reproduction and age-dependent senescence in L. japonicus

A role for SLs was postulated in reproduction, considering the high expression of *Arabidopsis MAX3* in siliques and seeds (Booker *et al*., 2004; Mashiguchi *et al*., 2009), of tomato *SlCCD7* in green immature fruits (Vogel *et al*., 2010), of *AcCCD7* and *AcCCD8* in young kiwifruits and seeds (Ledger *et al*., 2010), and of *ZmCCD8* in maize shank and ear shoots of female inflorescences (Guan *et al*., 2012). To date, however, CCD7 activity has never been proven to affect reproduction, and, more specifically, the reduced flower, fruit, and seed numbers observed in *L. japonicus* have never been reported for SL-depleted plants of any species. Rather, the petunia *dad1*/*ccd8* mutant is delayed in the setting of flowers, which also weigh less and are smaller than those of the wild type (Snowden *et al*., 2005). *SlCCD8*-silenced tomato plants also have smaller floral organs, fruits, and seeds, as well as 60% fewer seeds relative to controls (Kohlen *et al*., 2012). Also a significant reduction in the size and diameter of ear and shank was observed in maize *ZmCCD8* mutants (Guan *et al*., 2012). In contrast, abnormal floral organs, altered size and colour of flowers, pods, and seeds, or seed patterning inside the pod were not observed in transgenic Lotus consistent with the fact that no significant differences in free IAA content could be detected in flowers of RNAi and wild-type plants. Therefore, it is proposed that the observed reduction in seed production in transgenic plants is mainly due to the reduced number of flowers. To form its pseudoraceme inflorescences, the shoot main apex of *L. japonicus* produces a flower branch, which is subtended in the compound leaves and is terminated when one or two flowers are developed (Guo *et al*., 2006). A possible explanation for the reduced number of flowers in RNAi compared with transgenic control plants, in spite of their higher number of branches, is that their potential to form new buds that can produce flower branches may be reduced compared with controls. This, in turn, could be linked to the fact that the dormancy of many accessory buds was broken to give higher order branches, before transition from vegetative growth to flowering. Alternatively, or additionally, fewer resources could be available to reproduction in the SL-depleted plants because of the more vigorous vegetative growth (see below).

LjCCD7-silenced *Lotus* lines lagged in leaf senescence and abscission; this the first report linking senescence to a functional defect in a *CCD7* homologue. A correlation between SLs and senescence was instead reported in *Arabidopsis*, rice, and petunia plants lacking *MAX2* (Woo *et al*., 2001; Yan *et al*., 2007; Drummond *et al*., 2012), and in the *ccd8* mutants of petunia and kiwifruit (Snowden *et al*., 2005; Ledger *et al*., 2010). Transcripts of the *Arabidopsis MAX3*/*CCD7* and *MAX4*/*CCD8* genes accumulate during age-dependent leaf senescence, further suggesting that the role of SLs in the process may be direct (Breeze *et al*., 2011). However, mutation of the *MAX2* orthologue in pea (*RMS4*) does not affect leaf senescence (Johnson *et al*., 2006), implying that this is not a conserved feature of SLs across plant species.

A link may be seen between the delayed leaf senescence and impaired flower and seed production in the RNAi plants used here. Reproductive development controls the timing of leaf senescence, with photosynthates translocated from leaves to reproductive organs before death. The negative correlation between senescence and reproduction could be even more evident in polycarpic plants such as *L. japonicus*, which sets numerous inflorescences in subsequent rounds. The iterative production of reproductive organs and seeds may require more resources at the expense of vegetative fitness (Munné-Bosch, 2008). In this scenario, *LjCCD7*-silenced plants would allocate fewer resources than control plants to reproduction, thus delaying senescence and allowing higher biomass. This interpretation agrees with the observation that chlorophyll content was higher in the leaves of the RNAi lines used here compared with control plants, particularly at and after reproduction. It also agrees with the fact that total biomass was higher in RNAi plants than in controls. Whether the higher resource allocation to vegetative growth is the cause of the observed impairment of reproduction, or rather its effect, cannot be determined at this stage.

Role of SL in the regulation of root symbiosis in L. japonicus

The present data prove for the first time that SLs promote the formation of determinate nodules. The correlation between SLs and nodulation was previously investigated in *M. sativa* and pea, both forming indeterminate nodules (Soto *et al*., 2010; Foo and Davies, 2011; Foo *et al*., 2013). In *L. japonicus* as well, *LjCCD7*-silenced plants carried 20% fewer nodules than controls. As in the pea *rms1* mutant, alterations in nodule development and morphology were not detected. SLs apparently have no direct influence on the

growth of rhizobia, but they do have a quantitative effect on nodulation, in spite of their negative effect on the total root length and surface available to infection (Foo and Davies, 2011). Even if nodules and lateral roots form from different founder cells (being initiated by cortical versus pericycle cell divisions, respectively), a balance was proposed long ago to exist between nodule and lateral root formation, with nodule primordia initiation dependent on the suppression of lateral root emergence (Nutman, 1949). Later, it was proposed that the balance of auxin, cytokinins, and abscisic acid (ABA) decides the fate of pericycle cells and cortical cells, dictating whether lateral roots or nodules will be initiated (Ding and Oldroyd, 2009). Given the proven cross-talk of SLs with auxin (Crawford *et al*., 2010; Domagalska and Leyser, 2011; Ruyter-Spira *et al*., 2011; Kohlen *et al*., 2012) and ABA (Lechat *et al*., 2012; Toh *et al*., 2012), and the importance of both these hormones for normal frequency and development of determinate nodules in *Lotus* (Ding and Oldroyd, 2009), the phenotype observed in the SL-depleted plants could be auxin and/or ABA mediated, and be the outcome of an obviously defective suppression mechanism on lateral root emergence.

As proven for 5-deoxystrigol in root exudates of *L. japonicus* in the first place, SLs induce hyphal branching of AMF, increasing the chances of successful root colonization (Akiyama *et al*., 2005). A *MAX2*/*D3*-dependent, *D14*-independent effect on AMF colonization of roots was also observed very recently in rice (Yoshida *et al*., 2012). In an *SlCCD8*-knockdown line of tomato, ~50% reduction of total SLs in roots correlated with a 27% decrease in colonization by *Glomus intraradices* (Kohlen *et al*., 2012). Interestingly, the RNAi lines used in the present study did not show a significant reduction in AMF colonization for any of the parameters tested. Among all natural and synthetic SLs, 5-deoxystrigol (the only SL found in *Lotus*) is the most active, inducing AMF branching at subnanogram concentrations (Akiyama *et al*., 2010; Xie *et al*., 2010). Therefore, it is possible that the residual 20–30% of 5-deoxystrigol in the RNAi lines used here is still above the required threshold to induce fairly normal hyphal branching of *G. margarita* in our inoculation system (clean roots placed in close contact with germinating AMF spores). Very recently, protocols enabling highly efficient insertion mutagenesis were set up for *Lotus* (Fukai *et al*., 2012; Urbanski *et al*., 2012). The availability of such reverse genetic tools, through which complete knockout of genes would be achievable, will allow this point to be solved.

In summary, this is the first report of an SL-related phenotype in the perennial herbaceous model *L. japonicus*. Evidence was presented that *LjCCD7* is crucial for SL synthesis in *Lotus*, where the role of SLs is conserved in the regulation of root and shoot architecture, with some peculiarities; among them, the effects on primary root growth, internode length, number of higher order branches, and root-to-shoot biomass ratio. These apparent discrepancies are most probably specific features of SL action in the model plant used here, and, thus, just the reflection of biological diversity. Additional effects on reproduction and senescence were for the first time linked to an impairment in the expression of a CCD7 enzyme, and an effect of SLs on determinate nodulation was described. Further work is under way to unravel cross-talk of SLs with other hormones and their relative contributions to the observed phenotypes.

Supplementary data

Supplementary data are available at *JXB* online.

Figure S1. Phylogenetic analysis of CCD7 protein homologues.

Figure S2. LjCCD7 has carotenoid cleavage activity.

Figure S3. Representative comparison of high-order and basal shoot emergence between SL-depleted (RNAi) and negative transgenic control (NC) plants.

Figure S4. *LjCCD7* influence on reproduction.

Figure S5. *LjCCD7* impact on age-related senescence processes.

Table S1. List of primers used in this work.

Table S2. List of protein sequences used in phylogenetic analysis.

Acknowledgements

The authors wish to thank M. Chiurazzi (CNR, Italy) for suggestions about plant transformation, J. Stougaard (Aarhus University, Denmark) for Gifu B-129 seeds; S. Karunairetnam (Plant & Food Research, New Zealand) and R. Geurts (Wageningen University, The Netherlands) for vector pTKO2 and *Mesorhizobium loti*, respectively; W. Kohlen and I. Haider for their guidance during JL's. stay in Wageningen. Research was funded by the BioBITs Project [Piedmont Region, Converging Technologies 2007] to FC, AC, CL. and PB, and by the Netherlands Organization for Scientific Research [Vici grant, 865.06.002, 834.08.001] to HJB; JL was funded by the China Scholarship Council [2008108168].

References

Agusti J, Herold S, Schwarz M, *et al.* 2011. Strigolactone signaling is required for auxin-dependent stimulation of secondary growth in plants. *Proceedings of the National Academy of Sciences, USA* **108,** 20242–20247.

Akiyama K, Matsuzaki K, Hayashi H. 2005. Plant sesquiterpenes induce hyphal branching in arbuscular mycorrhizal fungi. *Nature* **435,** 824–827.

Akiyama K, Ogasawara S, Ito S, Hayashi H. 2010. Structural requirements of strigolactones for hyphal branching in AM fungi. *Plant and Cell Physiology* **51,** 1104–1117.

Alder A, Jamil M, Marzorati M, Bruno M, Vermathen M, Bigler P, Ghisla S, Bouwmeester H, Beyer P, Al-Babili S. 2012. The path from β-carotene to carlactone, a strigolactone-like plant hormone. *Science* **335,** 1348–1351.

Alvarez ND, Meeking RJ, White DWR. 2006. The origin, initiation and development of axillary shoot meristems in *Lotus japonicus*. *Annals of Botany* **98,** 953–963.

Arite T, Iwata H, Ohshima K, Maekawa M, Nakajima M, Kojima M, Sakakibara H, Kyozuka J. 2007. *DWARF10*, an *RMS1/MAX4/DAD1* ortholog, controls lateral bud outgrowth in rice. *The Plant Journal* **51,** 1019–1029.

Arite T, Kameoka H, Kyozuka J. 2012. Strigolactone positively controls crown root elongation in rice. *Journal of Plant Growth Regulation* **31,** 165–172.

Barbulova A, D'Apuzzo E, Rogato A, Chiurazzi M. 2005. Improved procedures for *in vitro* regeneration and for phenotypic analysis in the model legume *Lotus japonicus*. *Functional Plant Biology* **32,** 529–536.

Beveridge CA, Kyozuka J. 2009. New genes in the strigolactone-related shoot branching pathway. *Current Opinion in Plant Biology* **13,** 1–6.

Booker J, Auldridge M, Wills S, McCarty D, Klee H, Leyser C. 2004. MAX3/CCD7 is a carotenoid cleavage dioxygenase required for the synthesis of a novel plant signaling molecule. *Current Biology* **14,** 1232–1238.

Booker J, Sieberer T, Wright W, Williamson L, Willett B, Stirnberg P, Turnbull C, Srinivasan M, Goddard P, Leyser O. 2005. *MAX1* encodes a cytochrome P450 family member that acts downstream of *MAX3/4* to produce a carotenoid-derived branch-inhibiting hormone. *Developmental Cell* **8,** 443–449.

Bouwmeester HJ, Roux C, López-Ráez JA, Bécard G. 2007. Rhizosphere communication of plants, parasitic plants and AM fungi. *Trends in Plant Science* **12,** 224–230.

Breeze E, Harrison E, McHattie S, *et al.* 2011. High-resolution temporal profiling of transcripts during Arabidopsis leaf senescence reveals a distinct chronology of processes and regulation. *The Plant Cell* **23,** 873–894.

Broughton WJ, Dilworth MJ. 1971. Control of leghaemoglobin synthesis in snake beans. *Biochemical Journal* **125,** 1075–1080.

Crawford S, Shinohara N, Sieberer T, Williamson L, George G, Hepworth J, Muller D, Domagalska MA, Leyser O. 2010. Strigolactones enhance competition between shoot branches by dampening auxin transport. *Development* **137,** 2905–2913.

Cui HL, Wang YC, Qin S. 2012. Genomewide analysis of carotenoid cleavage dioxygenases in unicellular and filamentous cyanobacteria. *Comparative and Functional Genomics* **2012,** 1–13.

Delaux PM, Xie X, Timme RE, Puech-Pages V, Dunand C, Lecompte E, Delwiche CF, Yoneyama K, Bécard G, Séjalon-Delmas N. 2012. Origin of strigolactones in the green lineage. *New Phytologist* **195,** 857–871.

Ding Y, Oldroyd GE. 2009. Positioning the nodule, the hormone dictum. *Plant Signaling and Behavior* **4,** 89–93.

Domagalska MA, Leyser O. 2011. Signal integration in the control of shoot branching. *Nature Reviews Molecular Cell Biology* **12,** 211–221.

Drummond RS, Martínez-Sánchez NM, Janssen BJ, Templeton KR, Simons JL, Quinn BD, Karunairetnam S, Snowden KC. 2009. *Petunia hybrida CAROTENOID CLEAVAGE DIOXYGENASE 7* is involved in the production of negative and positive branching signals in petunia. *Plant Physiology* **151,** 1867–1877.

Drummond RS, Sheehan H, Simons JL, Martinez-Sanchez NM, Turner RM, Putterill J, Snowden KC. 2012. The expression of petunia strigolactone pathway genes is altered as part of the endogenous developmental program. *Frontiers in Plant Science* **2,** 115.

Foo E, Davies NW. 2011. Strigolactones promote nodulation in pea. *Planta* **234,** 1073–1081.

Foo E, Yoneyama K, Hugill C, Quittenden L, Reid J. 2013. Strigolactones and the regulation of pea symbioses in response to nitrate and phosphate deficiency. *Molecular Plant* **6,** 76–87.

Fukai E, Soyano T, Umehara Y, Nakayama S, Hirakawa H, Tabata S, Sato S, Hayashi M. 2012. Establishment of a *Lotus japonicus* gene tagging population using the exon-targeting endogenous retrotransposon *LORE1*. *The Plant Journal* **69,** 720–730.

Gomez-Roldan V, Fermas S, Brewer PB, *et al.* 2008. Strigolactone inhibition of shoot branching. *Nature* **455,** 189–194.

Guan JC, Suzuki M, Wu S, Latshaw SP, Petruff T, Goulet C, Klee HJ, Koch KE, McCarty DR. 2012. Diverse roles of strigolactone signaling in maize architecture and the uncoupling of a branching-specific sub-network. *Plant Physiology* **160,** 1303–1317.

Guo X, Zhao Z, Chen J, Hu X, Luo D. 2006. A putative *CENTRORADIALIS/TERMINAL FLOWER* 1-like gene, *LjCEN1*, plays a role in phase transition in *Lotus japonicus*. *Journal of Plant Physiology* **163,** 436–444.

Handberg K, Stougaard J. 1992. *Lotus japonicus*, an autogamous, diploid legume species for classical and molecular-genetics. *The Plant Journal* **2,** 487–496.

Hoagland A, Arnon D. 1950. The water-culture method for growing plants without soil. *California Agriculture Experiment Station Circular No. 347*.

Hu Z, Yan H, Yang J, Yamaguchi S, Maekawa M, Takamure I, Tsutsumi N, Kyozuka J, Nakazono M. 2010. Strigolactones negatively regulate mesocotyl elongation in rice during germination and growth in darkness. *Plant and Cell Physiology* **51,** 1136–1142.

Hwang I, Sheen J, Muller B. 2012. Cytokinin signaling networks. *Annual Review of Plant Biology* **63,** 353–380.

Johnson X, Brcich T, Dun EA, Goussot M, Haurogné K, Beveridge CA, Rameau C. 2006. Branching genes are conserved across species. Genes controlling a novel signal in pea are coregulated by other long-distance signals. *Plant Physiology* **142,** 1014–1026.

Kohlen W, Charnikhova T, Lammers M, *et al.* 2012. The tomato *CAROTENOID CLEAVAGE DIOXYGENASE 8* (*SlCCD8*) regulates rhizosphere signaling, plant architecture and affects reproductive development through strigolactone biosynthesis. *New Phytologist* **196,** 535–547.

Koltai H. 2011. Strigolactones are regulators of root development. *New Phytologist* **190,** 545–549.

Koltai H. 2012. Strigolactones activate different hormonal pathways for regulation of root development in response to phosphate growth conditions. *Annals of Botany* (in press).

Koltai H, Dor E, Hershenhorn J, *et al.* 2010*a*. Strigolactones' effect on root growth and root-hair elongation may be mediated by auxin-efflux carriers. *Journal of Plant Growth Regulation* **29,** 129–136.

Koltai H, LekKala SP, Bhattacharya C, *et al.* 2010*b*. A tomato strigolactone-impaired mutant displays aberrant shoot morphology

and plant interactions. *Journal of Experimental Botany* **61,** 1739–1749.

Lechat MM, Pouvreau JB, Peron T, *et al.* 2012. *PrCYP707A1*, an ABA catabolic gene, is a key component of *Phelipanche ramosa* seed germination in response to the strigolactone analogue GR24. *Journal of Experimental Botany* **63,** 5311–5322.

Ledger SE, Janssen BJ, Karunairetnam S, Wang T, Snowden KC. 2010. Modified *CAROTENOID CLEAVAGE DIOXYGENASE 8* expression correlates with altered branching in kiwifruit (*Actinidia chinensis*). *New Phytologist* **188,** 803–813.

Liang J, Zhao L, Challis R, Leyser O. 2010. Strigolactone regulation of shoot branching in chrysanthemum (*Dendranthema grandiflorum*). *Journal of Experimental Botany* **61,** 3069–3078.

Liu W, Kohlen W, Lillo A, *et al.* 2011. Strigolactone biosynthesis in *Medicago truncatula* and rice requires the symbiotic GRAS-type transcription factors NSP1 and NSP2. *The Plant Cell* **23,** 3853–3865.

Lohar DP, Bird DM. 2003. *Lotus japonicus*: a new model to study root-parasitic nematodes. *Plant and Cell Physiology* **44,** 1176–1184.

Lombari P, Ercolano E, El Alaoui H, Chiurazzi M. 2003. A new transformation–regeneration procedure in the model legume *Lotus japonicus*: root explants as a source of large numbers of cells susceptible to *Agrobacterium*-mediated transformation. *Plant Cell Reports* **21,** 771–777.

López-Ráez JA, Kohlen W, Charnikhova T, *et al.* 2010. Does abscisic acid affect strigolactone biosynthesis? *New Phytologist* **187,** 343–354.

Marasco EK, Vay K, Schmidt-Dannert C. 2006. Identification of carotenoid cleavage dioxygenases from *Nostoc* sp PCC 7120 with different cleavage activities. *Journal of Biological Chemistry* **281,** 31583–31593.

Mashiguchi K, Sasaki E, Shimada Y, Nagae M, Ueno K, Nakano T, Yoneyama K, Suzuki Y, Asami T. 2009. Feedback-regulation of strigolactone biosynthetic genes and strigolactone-regulated genes in Arabidopsis. *Bioscience, Biotechnology, and Biochemistry* **73,** 2460–2465.

Matusova R, Rani K, Verstappen FW, Franssen MC, Beale MH, Bouwmeester HJ. 2005. The strigolactone germination stimulants of the plant-parasitic *Striga* and *Orobanche* spp. are derived from the carotenoid pathway. *Plant Physiology* **139,** 920–934.

Mayzlish-Gati E, Lekkala SP, Resnick N, Wininger S, Bhattacharya C, Lemcoff JH, Kapulnik Y, Koltai H. 2010. Strigolactones are positive regulators of light-harvesting genes in tomato. *Journal of Experimental Botany* **61,** 3129–3136.

Morris SE, Turnbull CGN, Murfet IC, Beveridge CA. 2001. Mutational analysis of branching in pea. Evidence that *Rms1* and *Rms5* regulate the same novel signal. *Plant Physiology* **126,** 1205–1213.

Müller D, Leyser O. 2011. Auxin, cytokinin and the control of shoot branching. *Annals of Botany* **107,** 1203–1212.

Munné-Bosch S. 2008. Do perennials really senesce? *Trends in Plant Science* **13,** 216–220.

Ni Z, Kim ED, Chen ZJ. 2009. Chlorophyll and starch assays. *Protocol Exchange* DOI:10.1038/nprot.2009.1012.

Novero M, Faccio A, Genre A, Stougaard J, Webb KJ, Mulder L, Parniske M, Bonfante P. 2002. Dual requirement of the *LjSym4* gene for mycorrhizal development in epidermal and cortical cells of *Lotus japonicus* roots. *New Phytologist* **154,** 741–749.

Nutman PS. 1949. Physiological studies on nodule formation: I. The relation between nodulation and lateral root formation in red clover. *Annals of Botany* **13,** 261–283.

Proust H, Hoffmann B, Xie XN, Yoneyama K, Schaefer DG, Yoneyama K, Nogué F, Rameau C. 2011. Strigolactones regulate protonema branching and act as a quorum sensing-like signal in the moss *Physcomitrella patens*. *Development* **138,** 1531–1539.

Rasmussen A, Mason MG, De Cuyper C, *et al.* 2012. Strigolactones suppress adventitious rooting in Arabidopsis and pea. *Plant Physiology* **158,** 1976–1987.

Roose JL, Frankel LK, Bricker TM. 2011. Developmental defects in mutants of the PsbP domain protein 5 in *Arabidopsis thaliana*. *PLoS One* **6,** e28624.

Ruyter-Spira C, Kohlen W, Charnikhova T, *et al.* 2011. Physiological effects of the synthetic strigolactone analog GR24 on root system architecture in Arabidopsis: another belowground role for strigolactones? *Plant Physiology* **155,** 721–734.

Sachs T. 2005. Auxin's role as an example of the mechanisms of shoot/root relations. *Plant and Soil* **268,** 13–19.

Schwartz SH, Qin XQ, Loewen MC. 2004. The biochemical characterization of two carotenoid cleavage enzymes from Arabidopsis indicates that a carotenoid-derived compound inhibits lateral branching. *Journal of Biological Chemistry* **279,** 46940–46945.

Snowden KC, Simkin AJ, Janssen BJ, Templeton KR, Loucas HM, Simons JL, Karunairetnam S, Gleave AP, Clark DG, Klee HJ. 2005. The *Decreased apical dominance 1/Petunia hybrida CAROTENOID CLEAVAGE DIOXYGENASE 8* gene affects branch production and plays a role in leaf senescence, root growth, and flower development. *The Plant Cell* **17,** 746–759.

Sorefan K, Booker J, Haurogne K, *et al.* 2003. *MAX4* and *RMS1* are orthologous dioxygenase-like genes that regulate shoot branching in Arabidopsis and pea. *Genes and Development* **17,** 1469–1474.

Soto MJ, Fernández-Aparicio M, Castellanos-Morales V, García-Garrido JM, Ocampo JA, Delgado MJ, Vierheilig H. 2010. First indications for the involvement of strigolactones on nodule formation in alfalfa (*Medicago sativa*). *Soil Biology and Biochemistry* **42,** 383–385.

Sugimoto Y, Ueyama T. 2008. Production of (+)-5-deoxystrigol by *Lotus japonicus* root culture. *Phytochemistry* **69,** 212–217.

Toh S, Kamiya Y, Kawakami N, Nambara E, McCourt P, Tsuchiya Y. 2012. Thermoinhibition uncovers a role for strigolactones in Arabidopsis seed germination. *Plant and Cell Physiology* **53,** 107–117.

Trouvelot A, Kough JL, Gianinazzi-Pearson V. 1986. *Mesure du taux de mycorrhization VA d'un système radiculaire. Recherche de méthodes d'estimation ayant une signification fonctionnelle* . Paris: INRA Press, 217–222.

Tsuchiya Y, Vidaurre D, Toh S, Hanada A, Nambara E, Kamiya Y, Yamaguchi S, McCourt P. 2010. A small-molecule screen identifies new functions for the plant hormone strigolactone. *Nature Chemical Biology* **6,** 741–749.

Umehara M, Hanada A, Yoshida S, *et al.* 2008. Inhibition of shoot branching by new terpenoid plant hormones. *Nature* **455,** 195–200.

Urbanski DF, Malolepszy A, Stougaard J, Andersen SU. 2012. Genome-wide *LORE1* retrotransposon mutagenesis and high-throughput insertion detection in *Lotus japonicus*. *The Plant Journal* **69,** 731–741.

Vogel JT, Walter MH, Giavalisco P, *et al.* 2010. *SlCCD7* controls strigolactone biosynthesis, shoot branching and mycorrhiza-induced apocarotenoid formation in tomato. *The Plant Journal* **61,** 300–311.

Woo HR, Chung KM, Park JH, Oh SA, Ahn T, Hong SH, Jang SK, Nam HG. 2001. ORE9, an F-box protein that regulates leaf senescence in Arabidopsis. *The Plant Cell* **13,** 1779–1790.

Xie XN, Yoneyama K, Yoneyama K. 2010. The strigolactone story. *Annual Review of Phytopathology* **48,** 93–117.

Yan H, Saika H, Maekawa M, Takamure I, Tsutsumi N, Kyozuka J, Nakazono M. 2007. Rice tillering dwarf mutant *dwarf3* has increased leaf longevity during darkness-induced senescence or hydrogen peroxide-induced cell death. *Genes and Genetic Systems* **82,** 361–366.

Yokota K, Fukai E, Madsen LH, *et al.* 2009. Rearrangement of actin cytoskeleton mediates invasion of *Lotus japonicus* roots by *Mesorhizobium loti*. *The Plant Cell* **21,** 267–284.

Yoneyama K, Awad AA, Xie XN, Yoneyama K, Takeuchi Y. 2010. Strigolactones as germination stimulants for root parasitic plants. *Plant and Cell Physiology* **51,** 1095–1103.

Yoshida S, Kameoka H, Tempo M, Akiyama K, Umehara M, Yamaguchi S, Hayashi H, Kyozuka J, Shirasu K. 2012. The D3 F-box protein is a key component in host strigolactone responses essential for arbuscular mycorrhizal symbiosis. *New Phytologist* **196,** 1208–1216.

Zou J, Zhang S, Zhang W, Li G, Chen Z, Zhai W, Zhao X, Pan X, Xie Q, Zhu L. 2006. The rice *HIGH-TILLERING DWARF1* encoding an ortholog of Arabidopsis MAX3 is required for negative regulation of the outgrowth of axillary buds. *The Plant Journal* **48,** 687–698.